Eur. Phys. J. Appl. Phys. **89**, 10102 (2020)

https://doi.org/10.1051/epjap/2020190264

THE EUROPEAN PHYSICAL JOURNAL APPLIED PHYSICS

Regular Article

Study of nanocrystalline silicon-germanium for the development of thin film transistors★

Arturo Torres[1,*], Mario Moreno[1], Pedro Rosales[1], Miguel Dominguez[2], Alfonso Torres[1], Alfredo Morales[1], Adrian Itzmoyotl[1], and Javier de la Hidalga[1]

[1] National Institute of Astrophysics Optics and Electronics, INAOE, Puebla, Mexico
[2] Meritorious Autonomous University of Puebla, BUAP, Puebla, Mexico

Received: 2 September 2019 / Received in final form: 28 November 2019 / Accepted: 17 January 2020

Abstract. In this work, we study the effect of the deposition RF-power on the structural, optical and electrical properties of hydrogenated nanocrystalline silicon-germanium (nc-SiGe:H) thin films obtained by plasma enhanced chemical vapor deposition (PECVD) at substrate temperature of 200 °C. The objective is to produce films with high crystalline fraction in order to be used as active layers in thin film transistors (TFTs). Bottom-gate (BG) thin film transistors were fabricated with nc-SiGe:H active layers, deposited at different RF-power. Values of ON-OFF current ratio, subthreshold slope and threshold voltage of 10^5, 0.12 V/dec and 0.9 V, respectively, were obtained on TFTs with the nc-SiGe:H active layer deposited at 25 W.

1 Introduction

Thin film transistors based on hydrogenated amorphous silicon (a-Si:H) deposited by PECVD system have been used as low-cost switching elements in Active Matrix Liquid Crystal Displays (AMLCDs) [1]. However its low charge carrier mobility and its instability, resulted on devices with poor performance due to the creation of defects or charge trapping in the amorphous active layer [2]. The above make them unsuitable for large area and new electronic applications. Therefore, other semiconductor materials have replaced a-Si:H to be used as active layers in TFTs, such as hydrogenated microcrystalline silicon (μc-Si:H) which is obtained also by the PECVD technique. The main advantages of μc-Si:H over a-Si:H are its better electrical stability and higher charge carrier mobility [3].

As well, nc-SiGe:H TFTs have been developed, where a narrower and tunable band gap is achieved by adjusting the germane concentration, defined as $[GeH_4]/[GeH_4+SiH_4]$, during the PECVD deposition [4]. The nc-SiGe:H TFTs presents both, interface and bulk trap densities lower than μc-Si:H TFTs, resulting in a lower threshold voltage and subthreshold slope (faster commutation). Besides the above, ambipolarity has been observed in amorphous silicon-germanium (a-SiGe:H) TFTs [5].

In this work, we report the deposition and characterization nc-SiGe:H thin films obtained at different deposition RF-power by the PECVD technique, in order to be used as active layer in TFTs with BG structure. The undoped nc-SiGe:H thin films were deposited with gases mixture of SiH_4, GeH_4, H_2 and Ar, at a temperature and pressure of 200 °C and 1.2 Torr, respectively, while the deposition RF-power was varied from 10 to 25 W. The main objective is the correlation of the deposition RF-power with the films crystalline fraction and the TFTs performance.

2 Experimental

Undoped nc-SiGe:H thin films were obtained by PECVD system at standard RF frequency of 13.56 MHz, at 200 °C, with the objective to be used as active layers in TFTs. The films were deposited with a hydrogen flow (H_2) of 41 sccm, a silane (SiH_4) flow of 5 sccm and germane flow (GeH_4) also of 5 sccm (both SiH_4 and GeH_4 are diluted at 10% in H_2). The deposition RF-power was varied from 10 to 25 W, while the pressure in the chamber was maintained at 1.2 Torr. The deposition time was adjusted to obtain nc-SiGe:H thin films of about 100 nm. To form the source and drain contacts, a nc-Ge:H n-type film was deposited with the same temperature and pressure used for the deposition of intrinsic nc-SiGe:H film. The deposition was made with a H_2 flow of 20 sccm, a GeH_4 flow of 5 sccm (at 10% in H_2), and PH_3 flow of 15 sccm (at 1% in H_2).

In order to analyze the hydrogen bonding of silicon and germanium, Fourier Transform Infrared spectroscopy (FTIR) analysis was carried out with a BRUKER IR spectrometer (Vector 22) on films deposited on a n-type silicon wafer. Raman characterization was realized with a Horiba Jobin-Yvon (LabRam HR 800) spectrometer using a 632.8 nm laser. The optical band gaps were calculated through transmittance measurements in the range of 190–900 nm on Corning glass 1737 substrates by a Perkin-Elmer (Lambda Series) spectrometer. The activation energy and dark conductivity were estimated by means of electrical measurements made on Corning glass substrates with two

★ Contribution to the Topical Issue "Disordered Semiconductors: Physics and Applications", edited by Jean-Paul Kleider, Erik Johnson, Rudolf Brüggemann.

* e-mail: rturokts@hotmail.com

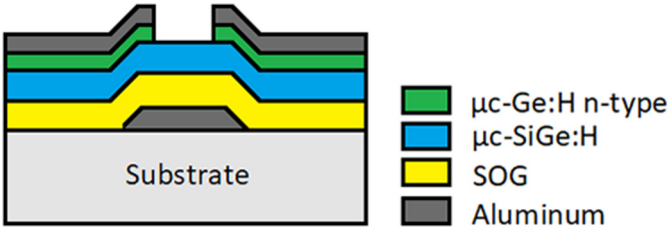

Fig. 1. Cross section of nc-SiGe:H TFT-BG fabricated.

thermally evaporated aluminum stripes, the gap between electrodes was 1.9 mm.

Figure 1 shows the cross-section of a nc-SiGe:H TFT-BG fabricated. As the first step, 100 nm of Al was evaporated on a Corning glass 2947 substrate, then the gate contact was formed by lithography (mask #1) and wet etching by Al-etch. As gate dielectric, Spin On Glass (SOG) diluted in deionized water (DI) with a proportion of 2:1 was deposited and cured for 6 h at 200 °C. After, the samples were transferred to the PECVD system for the sequential deposition of nc-SiGe:H and nc-Ge:H, to be used as active layer and n-type layer, respectively. Subsequently, 50 nm of Al was evaporated upon the n-type layer and by means of a lithographic step (mask #2), the source and drain contacts were formed by Al-etch. A lithographic step (mask #3) and an etching step by Reactive Ion Etching (RIE) were made to selectively etch the n-type layer, the active layer and the dielectric layer, in order to have electrical contact to the gate and isolate each TFT. Finally, the source and drain contacts are used as masks to etch the n-type layer between contacts. The transfer characteristics of TFTs with channel widths (W) of 140, 160, 140, 120 and channel length (L) of 20, 20, 30, 40 fabricated at 10, 15, 20 and 25 W, respectively, and output characteristic of TFT with $W/L = 160/30$, $160/20$, $140/30$ and $180/20$ of TFTs deposited at RF-power of 10, 15, 20 and 25 W, respectively, was carried out using a Keithley 4200 parameter analyzer.

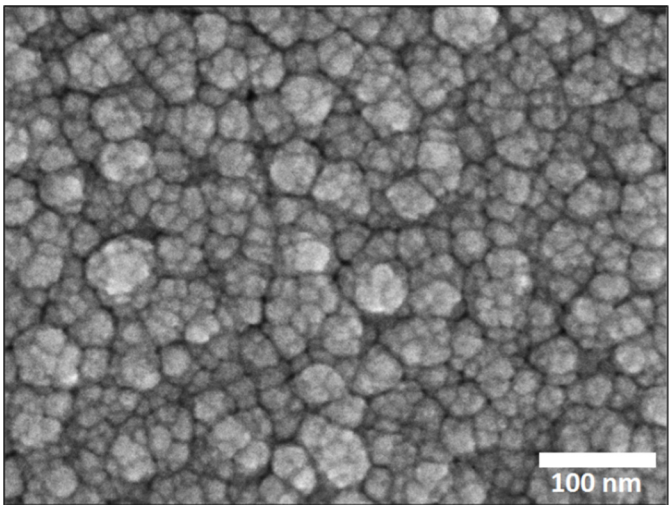

Fig. 2. FE-SEM image of the surface of a nc-SiGe:H film.

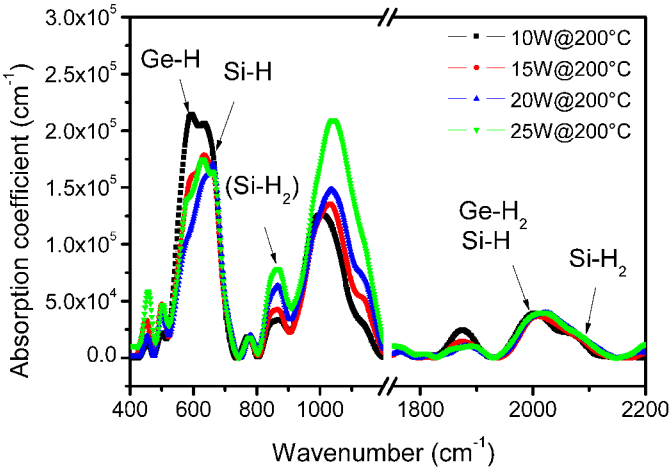

Fig. 3. IR spectra of nc-SiGe:H thin films deposited at different RF-power.

3 Results and discussion

3.1 nc-SiGe:H thin films characterization

Figure 2 shows a field emission scanning electron microscope (FE-SEM) image of the surface of a nc-SiGe:H film deposited at a RF power of 25 W. In the figure is possible to observe grains of sizes in the range of 30–50 nm. The film does not have any covering and therefore it is possible observe more details in the nanograins that compose the film.

The FTIR spectra is used to investigate the configuration and estimate the concentration of hydrogen bonds in the films. The FTIR absorption spectra of the nc-SiGe:H thin films obtained at different RF-power is shown in Figure 3. In the figure, bands of absorption of Ge–H and Si–H bonds can be observed in 560 cm^{-1} and 640 cm^{-1}, respectively, both in wagging mode [6]. The peak at 890 cm^{-1} corresponds to the bending mode of $(Si\text{-}H_2)n$ [7]. We also can see around 1000–1040 cm^{-1} a peak belonging to Si–O–Si stretching mode [8]. According to mentioned by Li et al. [9] this indicates an increase of microvoids in the films, therefore the films tend to oxidize more as the deposition RF-power increases. Furthermore, absorption peaks in stretching mode of Si-H and $Si\text{-}H_2$ bonds are observed in 2000 cm^{-1} and 2100 cm^{-1}, respectively, while the Ge-H and $Ge\text{-}H_2$ bonds are observed in 1890 cm^{-1} and 2000 cm^{-1}, respectively [6,10].

The bands close to 580 cm^{-1} and 640 cm^{-1} assigned to the Ge–H and Si–H bonds, respectively, are used to calculate the hydrogen content (C_H) by means of the following relations (Eqs. (1) and (2)) [11]:

$$N(\mathrm{cm}^3) = A \int \frac{\alpha(\omega)}{\omega} \mathrm{d}\omega, \tag{1}$$

$$C_H = \frac{N(\mathrm{Cm}^3)}{\rho} \times 100, \tag{2}$$

where ρ is the atomic density of Si or Ge, $\alpha(\omega)$ is the absorption coefficient at the frequency ω, A is the factor of proportionality, $A = 1.6 \times 10^{19}$ cm^{-2} for Si and $1.1 \times$

Table 1. Values of hydrogen content of Ge-H and Si-H bonds at 580 cm^{-1} and 640 cm^{-1}, respectively.

Sample	$C_{H(580)}$ (%) Ge-H	$C_{H(640)}$ (%) Si-H
10 W@200 °C	6.7	5.8
15 W@200 °C	4.4	4.9
20 W@200 °C	3.2	4.8
25 W@200 °C	3.1	4.1

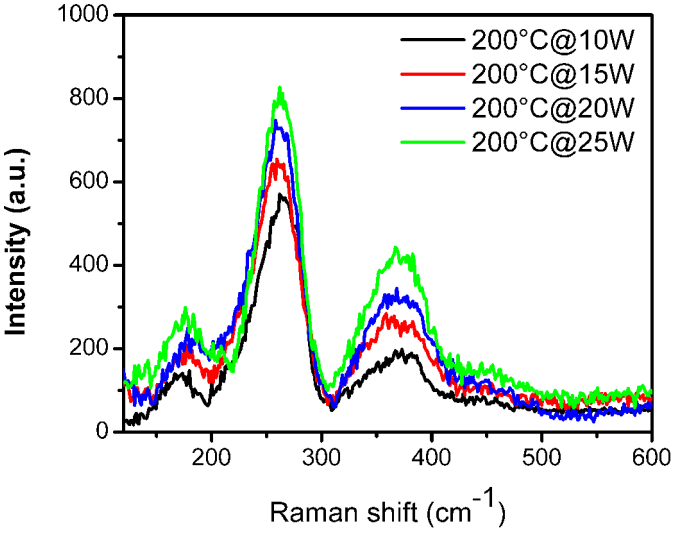

Fig. 4. Raman spectra of nc-SiGe:H thin films.

10^{19} cm^{-2} for Ge [8]. Table 1 shows the hydrogen content values calculated of Ge-H and Si-H bonds near of 580 cm^{-1} and 640 cm^{-1} bands, respectively. With the increase of deposition power, there is a reduction of C_H. A lower concentration of Ge-H ($C_{H(580)}$) and Si-H ($C_{H(640)}$) bonds is related to the reduction of the amorphous phase in the films since the H atoms will be located mainly at the grain boundaries regions in the form of Si-H_2 bonds [12] as can be seen in the 890 cm^{-1} and 2100 cm^{-1} bands.

The Raman spectra of nc-SiGe:H thin films obtained at different RF-power is shown in Figure 4. Transversal optic (TO) modes of vibration of Ge-Ge, Si-Ge bonds at approximately 280 cm^{-1} and 390 cm^{-1}, respectively, are observed. The peak assigned to the Ge–Ge bonds has shifted towards smaller wave numbers due to the surrounding presence of silicon bonds [13]. The band belonging to the Si-Si bond can be seen as a broad peak around 450 cm^{-1} which indicates an amorphous part in the films. Even though the films were deposited with the same SiH_4 and GeH_4 flow rates, there was a larger content of Ge atoms than Si atoms in the films. The above is consequence of a larger reactive Ge species than Si species in the plasma, due to the lower binding energy of the GeH_4 molecules than that of SiH_4 molecules. In the Raman spectra is also observed that the peak of the Ge-Ge bonds increases with the deposition RF-power, which is an indication of the crystalline fraction in the films.

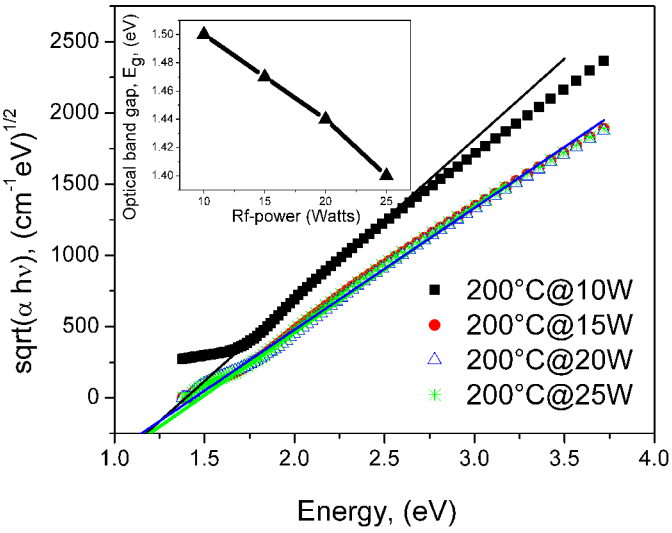

Fig. 5. Optical band gap obtained from Tauc method of nc-SiGe:H thin films. Inset of figure shows the optical band gap as a function of deposition RF-power.

Through of UV–Vis transmittance measurements in the region of 190–900 nm the optical band gaps (E_g) were calculated using the Tauc method [14], where E_g is obtained using the following relation (Eq. (3)):

$$(\alpha h\nu)^{1/2} = B(h\nu - E_g) \tag{3}$$

where α is the absorption coefficient, h is the Planck's constant, ν is the photon frequency and B is a proportionality constant. In Figure 5 it has been plotted $(\alpha h\nu)^{1/2}$ *vs* the photon energy, where E_g is obtained by extrapolating the linear part of $(\alpha h\nu)^{1/2}$ to $\alpha = 0$. In the inset of Figure 5 the optical band gap values have been plotted as a function of the deposition RF-power and is observed that E_g decreases from 1.50 eV to 1.40 eV by increasing the deposition RF-power from 10 to 25 W.

The activation energy (E_a) of the films was obtained by measuring the conductivity as a function of temperature in a range of 300–400 K. The temperature-dependent conductivity and E_a are related by the Arrhenius type equation (Eq. (4)), where σ_T is the conductivity as a function of temperature, K the Boltzman constant, T the temperature and σ_0 a constant. The activation energy is the value of the slope of the graph $\ln(\sigma_T)$ vs 1/KT.

$$\sigma = \sigma_0 \exp(-E_A/KT). \tag{4}$$

Figure 6 shows E_A as a function of the deposition RF-power. As can be seen, E_A decreases monotonously from 0.66 eV to 0.44 eV as the RF-power increases. Figure 6 also presents the dark conductivity (σ_d) as a function of RF-power. In this case, the conductivity increased two orders of magnitude by increasing the deposition RF-power. The conductivity of the film at 10 W was 1.8×10^{-9} Ω^{-1} cm^{-1} and 3.2×10^{-7} Ω^{-1} cm^{-1} for the film obtained at 25 W. The increase in conductivity can be explained based both, on the fact that raising the

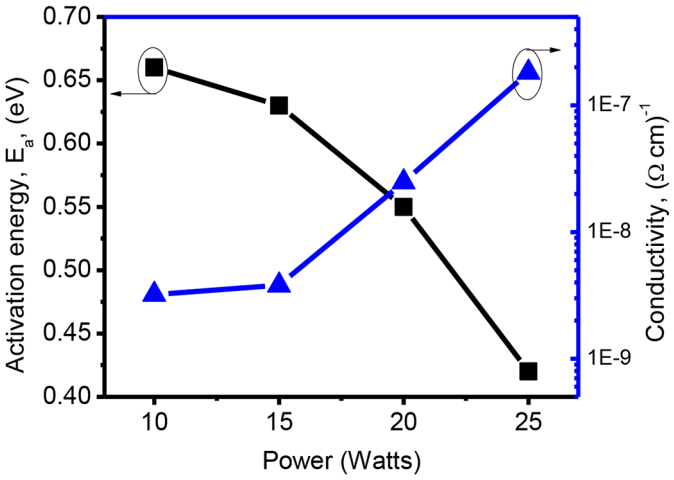

Fig. 6. Activation energy (E_a) and dark conductivity both as function of deposition RF-power.

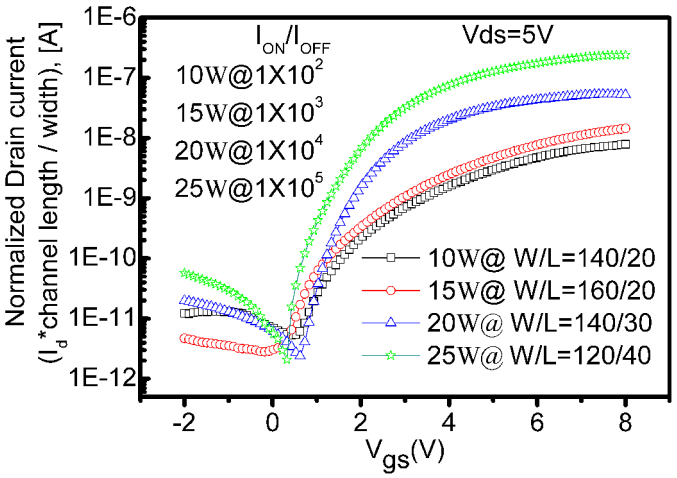

Fig. 7. Normalized transfer characteristics in the saturation region (Vds = 5 V) of TFT with different widths and channel lengths.

crystalline fraction of the films the mobility of the carriers will be larger and consequently the conductivity, and to a decrease in the states density in the band gap with the deposition RF power. At low negative voltage bias, most of the electrons injected in the semiconductor are trapped into localized states (deep and tail states) in the band gap. The deep states are filled first and the fermi level moves through those states. As the negative voltage bias increase, the fermi level approaches the conduction band edge as more traps are filled. At an adequately high voltage, all tail states are filled, thus increasing exponentially the free electron density.

3.2 TFTs characterization

The electrical characteristics of the TFTs were measured at room temperature and in dark conditions. Figure 7 shows the normalized (drain current x channel length/width) transfer characteristics in the saturation region ($V_{ds} = 5V$) of TFTs with different W and L ratios. An ON-OFF current ratio of 10^5, 10^4, 10^3 and 10^2 was obtained for the TFT with active layer deposited at 25, 20, 15 and 10 W, respectively.

The increment of the ON-OFF current ratio can be explained by the increase of the crystalline fraction of the nc-SiGe:H active layer of the TFTs. The growth process of nc-SiGe:H films begins with an amorphous incubation layer and depending on the deposition conditions, the bulk layer can contain a few concentrations of nanocrystals or microcrystalline columns. When the film is highly crystalline, the incubation film thickness is reduced. One of the most important parameters for grow films with high crystalline fraction is precisely the RF-power, usually larger RF-power results in films with larger crystalline fraction. In a TFT with BG structure, the channel is formed at the bottom of the thin film, therefore, by decreasing the incubation layer and increasing the crystalline fraction a material with fewer defects is obtained, in this way there will be a higher concentration of carriers forming the channel, and consequently increasing the current of the device.

The subthreshold swing ($S = dV_g/d(Log\,(I_g))$ defined as the maximum slope of the transfer curve was also obtained from this graph. The values of S were 0.8, 0.48, 0.30 and 0.12 V/dec for TFT with active layer deposited with RF-power of 10, 15, 20 and 25 W, respectively. The decrement in the subthreshold swing with the increase in the crystalline fraction indicates a decrease in defects in the active layer of the TFT because the subthreshold slope is directly related to the density of defects in the channel [15]. The threshold voltage (V_T) was estimated of the graph $(I_d)^{1/2} vs\, V_{gs}$ (not shown here), that is, when the TFT operates in saturation mode. V_T defined as the x-axis intercept of straight line extrapolating from a linear portion of $(I_d)^{1/2} vs\, V_{gs}$. The calculated V_T was 1.1, 1.2, 1.26 and 0.94 V for the TFTs fabricated at RF-power of 10, 15, 20 and 25 W, respectively.

Figure 8a–d shows the output characteristic of TFT with $W/L = 160/30$, 160/20, 140/30 and 180/20 of TFTs with active layer deposited at RF-power of 10, 15, 20 and 25 W, respectively. As we can see, the output characteristic has a clear saturation regime, although current crowding effects at low drain voltages (Vds < 0.5 V) are observed, which could be due to a high resistance of the source and drain contacts [16], analysis of current crowding is described elsewhere [17].

4 Conclusions

In this work, we have reported the structural, optical and electrical characterization of nc-SiGe:H thin films obtained by the PECVD system. Moreover, we present how the deposition RF-power of the active layer affects the performance of TFTs with bottom gate structure. Values of on-off current ratio of 10^2, 10^3, 10^4 and 10^5 and subthreshold slope values of 0.8, 0.48, 0.30 and 0.12 V/dec were calculated for TFTs with active layer deposited at RF-power of 10, 15, 20 and 25 W, respectively. Therefore, by rising the deposition RF power of the nc-SiGe:H thin films there is an increase of ON current and, consequently, a higher ON/OFF ratio of the fabricated TFTs.

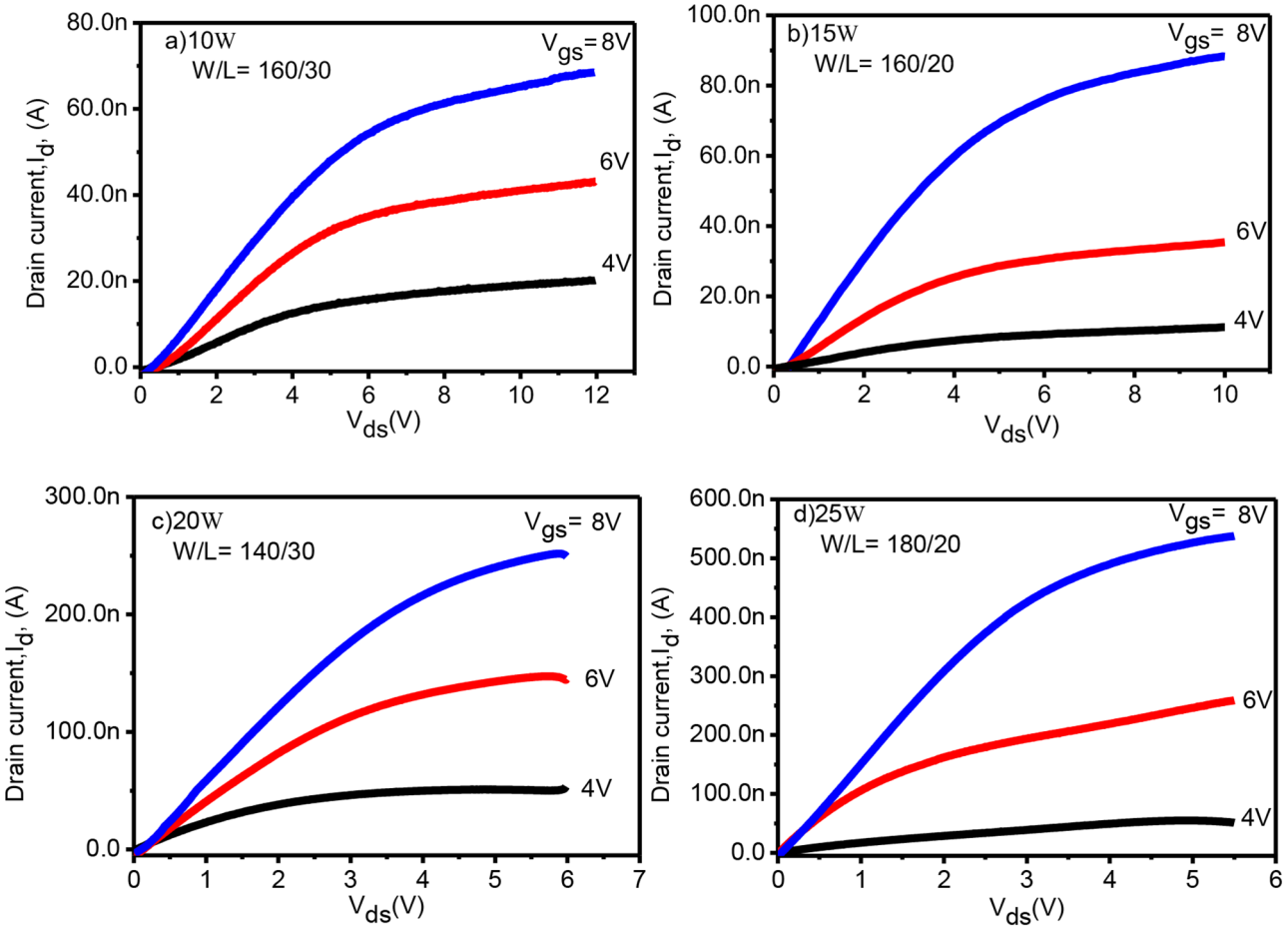

Fig. 8. (a)–(d) Output characteristic of TFT with W/L = 160/30, 160/20, 140/30 and 180/20 of nc-SiGe:H TFTs.

Arturo Torres acknowledges to the National Council of Science and Technology of Mexico, CONACYT, for its support for this work through a PHD scholarship.

Author contribution statement

Arturo Torres, Mario Moreno and Pedro Rosales designed, planned and performed the experiment of deposition thin films. Miguel Dominguez, Alfonso Torres, Alfredo Morales and Javier de la Hidalga supervised, reviewed and evaluated the results of the characterization of TFTs. Adrian Itzmoyotl performed the thin films deposition by PECVD system. Arturo Torres and Mario Moreno wrote the manuscript with collaboration of Pedro Rosales and Miguel Dominguez.

References

1. M. Dominguez et al., J. Thin Solid Films **562**, 260 (2014)
2. C.Y. Ho, Y.J. Chang, Solid State Electron. **116**, 130 (2016)
3. K.Y. Chan et al., Solid State Electron. **52**, 914 (2008)
4. Y.T. Huang et al., Int. J. Photoenergy **2014**, 1 (2014)
5. M. Dominguez et al., J. Non Cryst. Solids **358**, 2340 (2012)
6. S. Kim, C. Park, J.C. Lee, J.S. Cho, Y. Kim, J. Thin Solid Films **534**, 214 (2013)
7. B. Yan et al., J. Vacuum **89**, 43 (2013)
8. Y.P. Chou, S.C. Lee, J. Appl. Phys. **83**, 4111 (1998)
9. T. Li et al., J. Optoelectron. Lett. **10**, 202 (2014)
10. S. Kim et al., J. Curr. Appl. Phys. **13**, 457 (2013)
11. R. Xu, W. Li, J. He, Y. Sun, Y.D. Jiang, J. Non Cryst. Solids **365**, 37 (2013)
12. T. Anutgan, M. Anutgan. I. Atilgan, B. Katircioglu, J. Vacuum **85**, 875 (2011)
13. G. Ganguly et al., J. Appl. Phys. Lett. **69**, 4224 (1996)
14. G. Wang et al., J. Thin Solid Films **659**, 36 (2018)
15. K. Chan, A. Gordijn, H. Stiebig, D. Knipp, IEEE Trans. Electr. Dev. **56**, 1924 (2009)
16. M.A. Dominguez et al., J. Thin Solid Films **619**, 261 (2016)
17. P. Zhang et al., J. Phys. D: Appl. Phys. **48**, 475501 (2015)

Cite this article as: Arturo Torres, Mario Moreno, Pedro Rosales, Miguel Dominguez, Alfonso Torres, Alfredo Morales, Adrian Itzmoyotl, Javier de la Hidalga, Study of nanocrystalline silicon-germanium for the development of thin film transistors, Eur. Phys. J. Appl. Phys. **89**, 10102 (2020)